We are IntechOpen, the world's leading publisher of Open Access books Built by scientists, for scientists

4,800
Open access books available

122,000
International authors and editors

135M
Downloads

Our authors are among the

154
Countries delivered to

TOP 1%
most cited scientists

12.2%
Contributors from top 500 universities

CLARIVATE ANALYTICS BOOK CITATION INDEX INDEXED

WEB OF SCIENCE™

Selection of our books indexed in the Book Citation Index in Web of Science™ Core Collection (BKCI)

Interested in publishing with us?
Contact book.department@intechopen.com

Numbers displayed above are based on latest data collected.
For more information visit www.intechopen.com

11

Directional Tuning Control of Wireless/Contactless Power Pickup for Inductive Power Transfer (IPT) System

Jr-Uei William Hsu, Aiguo Patrick Hu and Akshya Swain
The University of Auckland
New Zealand

1. Introduction

Inductive Power Transfer (IPT) systems have successfully been developed and used to replace traditional conductive power transfer systems where physical connection is either inconvenient or impossible, such as biomedical implants, undersea vehicles, and contactless battery chargers of robots, for providing power to movable or detachable loads (Kim et al., 2001; Feezor et al., 2001; Harrison, 2007). As IPT systems extend to more fields, better control methods are required to cope with various operating environments to satisfy users' needs. Difficulties in controlling the power flow in a wireless/contactless power pickup using IPT technologies can arise from several factors, which include but not limited to load and circuit parameter variations, magnetic field coupling variations between the primary and secondary coils, the operating frequency drift of the primary power supply, etc (Jackson et al., 2000; Chao et al., 2007). These factors can cause the output voltage of the secondary power pickup to deviate significantly from the original designed value, resulting in an undesirable characteristic for applications where a stable output voltage is required. Hence, there is a need to develop controllers under various operating conditions.

Practical power flow control of an IPT sytem can generally be categorized into three different types: namely, primary power supply control, secondary power pick-up control, and coordinated control of both primary and secondary circuits. Among these three, direct power flow control at secondary power pickups is most commonly used to stabilize the output voltage, paricularly for multiple power pickup applications (Hu et al., 2007; Wang et al., 2006; Gao, 2005). This chapter presents the basic theory and control algotithm of an improved directional tuning control method for power flow control of secondary contactless/wireless power pickup circuits.

2. Background of Inductive Power Transfer (IPT) system

The basic structure of an IPT system is shown in Fig. 1 (Wang et al., 2000; Wang et al., 2005; Bieler et al., 2002). The system comprises two electrically isolated parts: the primay power supply and the secondary power pickup. The primary power supply is normally stationay and consists of a resonant power supply and an elongated conductive path for producing a constant AC track current. The secondary movable part, also called the power pickup, is mutually coupled with the primary track and moves with respect to the track loop as the

Source: Advances in Solid State Circuits Technologies, Book edited by: Paul K. Chu,
ISBN 978-953-307-086-5, pp. 446, April 2010, INTECH, Croatia, downloaded from SCIYO.COM

operation requires. Since the system is often loosely coupled between its primary and secondary side, the induced voltage source is usually unsuitable for direct use in applications. As a result, proper tuning and control are essential in the system design for providing a constant DC voltage to the load.

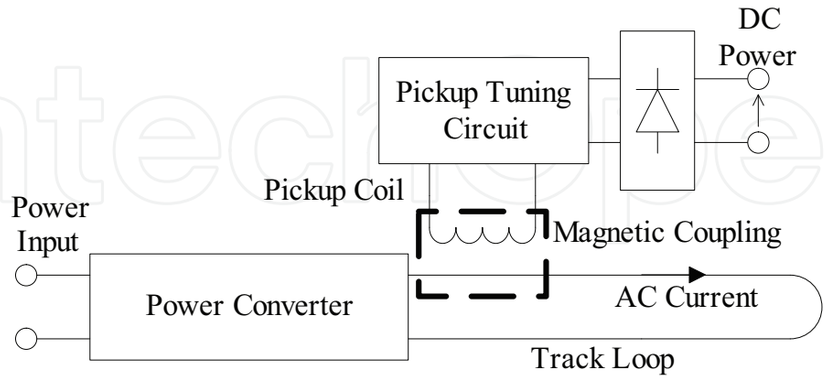

Fig. 1. Basic structure of an IPT system with uncontrolled power pickup.

Figure 2. shows the structure of a typical IPT power pickup. L_S and C_S represent the secondary pickup coil inductance and tuning capacitance respectively, a parallel tuning configuration is adopted here for boosting the induced open circuit voltage.

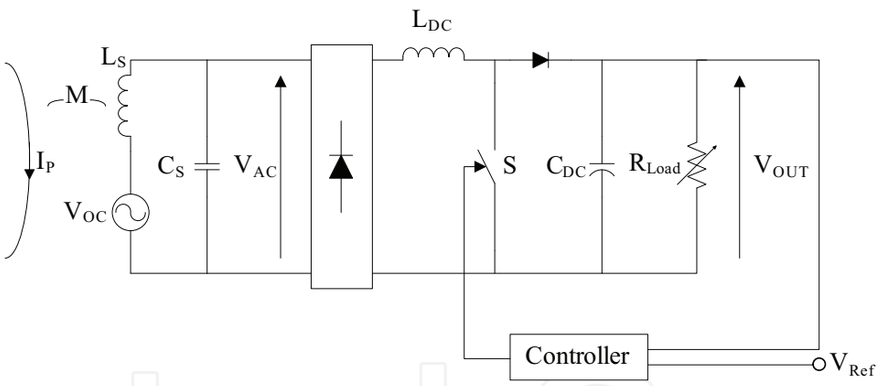

Fig. 2. Basic structure of an IPT power pickup with shorting-control.

The open circuit voltage V_{OC} and short circuit current (I_{SC}) of the pickup coil are governed by the following equations:

$$V_{OC} = j\omega M I_P \tag{1}$$

$$I_{SC} = {V_{OC}}/{j\omega L_S} \tag{2}$$

In Figure 2 the voltage V_{AC} after tuning is converted from AC to DC through rectifiers to provide a DC output voltage V_{OUT}. To simply the analysis, the rectifier and load can be represented with the equivalent AC resistor R_{AC}. The transfer function of the system given in (3) can be derived from the simplified second order system shown in Fig. 3, and it also can be seen that at steady state the pickup provides a current source to the load when it is fully-tuned.

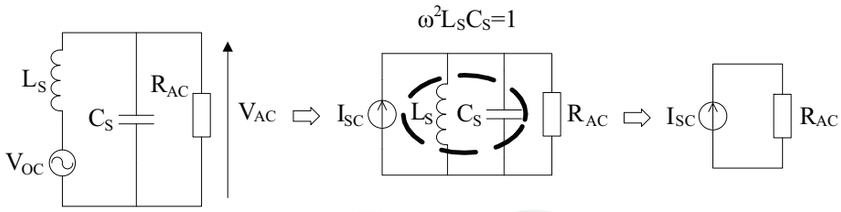

Fig. 3. Simplified second order tuning circuit of power pickup.

$$\frac{V_{AC}}{V_{OC}} = \frac{1/L_S C_S}{s^2 + 1/R_{AC} C_S \, s + 1/L_S C_S} \tag{3}$$

where ω is the system operating frequency. The maximum voltage boost-up factor of power pickup is gorverned by Q factor of the tuning circuit, and under fully-tuned condition it can be expressed as:

$$k_v = \left| \frac{V_{AC}}{V_{OC}} \right| = \frac{R_{AC}}{\sqrt{\left[R_{AC} \left(1 - \omega^2 L_S C_S \right) \right]^2 + \left(\omega L_S \right)^2}} \tag{4}$$

$$Q = k_{v\max} = \frac{R_{AC}}{\omega L_S}, \quad if \quad \omega^2 L_S C_S = 1 \tag{5}$$

The AC equivalent load resistance R_{AC} is given by:

$$R_{AC} = \frac{\pi^2}{8} R_{Load} \tag{6}$$

where R_{Load} is the DC load resistance. A DC inductor L_{DC} is normally added after the rectifier to maintain a continuous current flow, so that the available power of the secondary pickup can be fully delivered to the load. The output voltage regulation is normally achieved by using a well-known control technique called "Shorting-Control" (Boys et al., 2000; Elliot et al., 1995; Raabe et al., 2007). Its working principle is similar to a boost converter. The constant output voltage is maintained by controlling the average current flowing through the load by switching a semiconductor device (S, shown in Fig. 2) on and off using either hysteresis or PWM control. However, this controller cannot maintain the full-tuning condition of the secondary power pickup circuit. Therefore, the maximum power which can be transferred may be significantly reduced if the circuit parameters vary. And due to the fact that the short circuit current of the pickup coil has to flow through the switch during shorting period, which causes high power losses particularly under light loading conditions, this shortcoming also decreases the potential capability of the primary power supply to operate with more pickups due to unnecessary power loss and possible circuit mistuning.

An alternative method that has been investigated to further improve the power flow control is the dynamic tuning/detuning technique (Hu et al., 2004; Si et al., 2006). Figure 4 shows the general structure of dynamic tuning/detuning control scheme. The fundamental concept of this control method is to dynamically change the tuning condition of the power pickup according to the actual load demands. This helps to maintain maximum power transfer

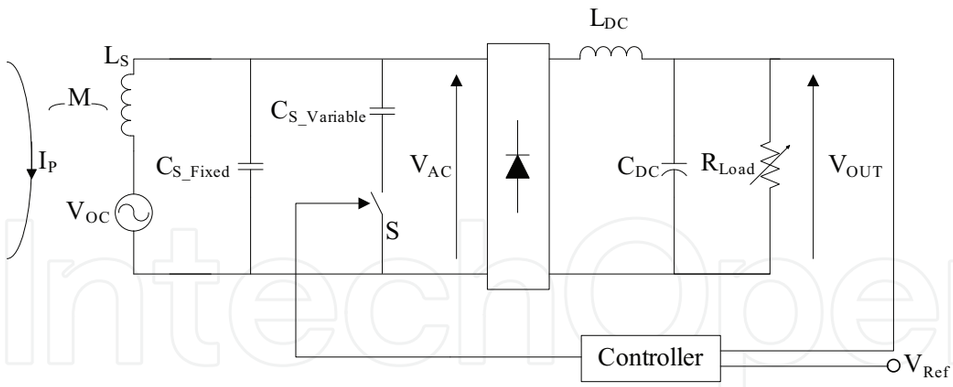

Fig. 4. Basic structure of an IPT power pickup with dynamic tuning/detuning control.

capacity, improve the overall efficiency of the system under light loading condition while keeping the output voltage to be constant. The control strategy is achieved by using a PI controller to control the on/off time of a soft-switched tuning inductor/capacitor to obtain the desired values of equivalent inductance/capacitance in the resonant tank. However, because the relationship between the tuning components and the output voltage is bell-shaped (shown in Fig. 5), there are two possible operating points with one in the over-tuned region and the other in under-tuned region. If the operating point has been accidentally shifted to the other region due to variations of circuit parameters, the desired equivalent values may be tracked in the wrong direction and consequently fail to control the output voltage.

To overcome the problems associated with existing control methods of power pickups such as shorting control, dynamic tuning/detuning control, etc., an LCL (Inductor-Capacitor-Inductor) based power pickup with directional tuning control (DTC) algorithm is proposed and has been discussed in detail in this chapter. Its working principle is similar to the dynamic tuning/detuning control technique. However, instead of using the traditional PI controller to perform the tracking process, it uses the present and previous control results to determine the correct tracking direction in the next step, and retune the circuit to deliver the required power (Hsu et al., 2006). Such an approach covers the full-tuning curve, so dual-side (full-range) control can be achieved. The proposed controller can provide reliable

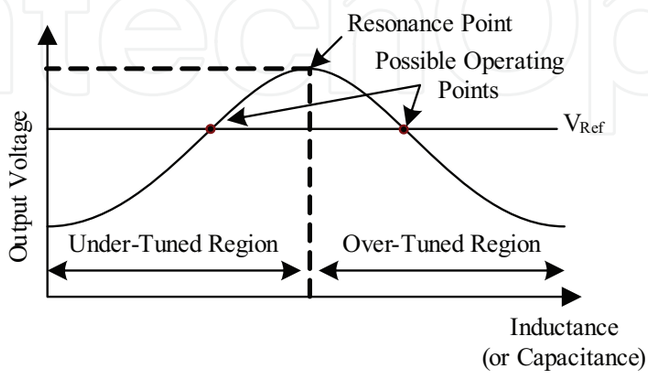

Fig. 5. Relationship between tuning inductance/capacitance and output voltage of IPT power pickup.

constant output voltage under various circuit parameter variations, thus eliminating the need for tedious fine-tuning process required by traditional IPT pickups. As a result, it is more cost-effective for mass production with reduced tuning and component tolerance requirements.

3. Effects of power pickup parameter variations on output voltage

In practical operations, the pickups are often deviated from its designated operating point due to the variation of circuit parameters. Since the deviation of output voltage may not be regulated by the general controller, especially under full-tuning range, the effect of each parameter variation on the output voltage is therefore need to be individually examined so the control range based on the given maximum tolerance to pickup parameters can be better understood (Hsu et al., 2007). The considered circuit parameters include: system operating frequency, magnetic coupling between the primary and secondary side, load resistance and tuning capacitance. Figure 6 shows the structure of the proposed secondary power pickup. An LCL tuning configuration is being used here to provide a constant output voltage to the load under resonant conditions, and a magnetic amplifier in the tuning circuit serves as a variable inductor for changing the tuning condition of the power pickup. The DC current (I_{MA}) which controls the magnetic amplifier is varied through a transistor operating in linear mode which essentially functions as a variable resistor. The equivalent inductance of L_{S2} is adjusted through changing the output signal V_{ctrl} from the DTC algorithm, which allows the power pickup to deliver the right amount of power required by the load (Hsu et al., 2009).

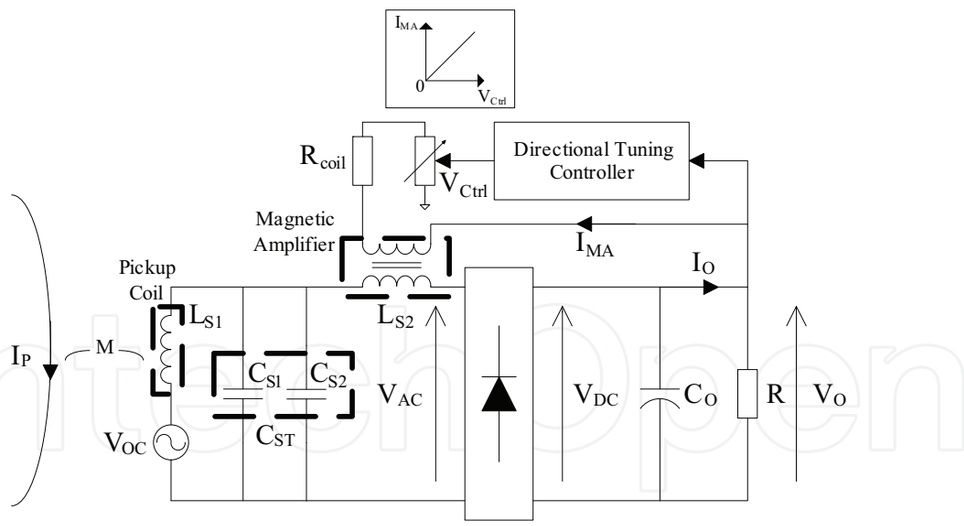

Fig. 6. The proposed LCL power pickup with directional tuning control.

The boost-up factors for ac voltage (V_{AC}) and current (I_{AC}) of the LCL tuning circuit can be determined from the following two transfer functions.

$$k_v = \frac{V_{AC}}{V_{OC}} = \frac{R \big/ L_{S1}L_{S2}C_{ST}}{s^3 + \frac{R}{L_{S2}}s^2 + \frac{L_{S1}+L_{S2}}{L_{S1}L_{S2}C_{ST}}s + \frac{R}{L_{S1}L_{S2}C_{ST}}} \tag{7}$$

$$k_i = \frac{I_{AC}}{I_{SC}} = \frac{sL_{S1}}{R} \cdot \frac{V_{AC}}{V_{OC}} \tag{8}$$

As shown in Fig. 6, the value of C_{ST} can be separated into C_{S1} and C_{S2} which resonate respectively with L_{S1} and L_{S2} *i.e.* $j\omega L_{S1}C_{S1} = j\omega L_{S2}C_{S2} = 1$. The ac voltage boost-up factor k_r under full resonant condition can be expressed as:

$$k_r = \frac{V_{AC}}{V_{OC}} = \frac{L_{S2}}{L_{S1}} = \frac{C_{S1}}{C_{S2}} \tag{9}$$

With the considered circuit parameters, the magnitude of AC boost-up factor k_v in (7) can be further expressed as:

$$k_{vm} = \frac{\alpha_v \alpha_f \alpha_r k_r R}{\sqrt{\left\{\alpha_r R\left[\alpha_f{}^2 \alpha_c (k_r + 1) - k_r\right]\right\}^2 + \left\{\omega\left[k_r L_{S1} - \left[\alpha_f{}^2 \alpha_c (k_r + 1) - k_r\right] L_{S2}\right]\right\}^2}} \tag{10}$$

where α_v, α_r, α_f, and α_c is the per unit variation of open circuit voltage, load resistance, primary operating frequency, and tuning capacitance, respectively and these are equal to unity when they are at their nominal values. For example if the open circuit voltage increases or decreases by 10%, the value of α_v is set to 1.1 or 0.9 respectively. By rearranging (10) into a quadratic equation of L_{S2}, the solution can be obtained as:

$$L_{S2} = \frac{k_r L_{S1}}{\alpha_f{}^2 \alpha_c (k_r + 1) - k_r} \pm \frac{\alpha_r R \sqrt{\left(\alpha_v \alpha_f k_r\right)^2 - \left\{k_{\min}\left[\alpha_f{}^2 \alpha_c (k_r + 1) - k_r\right]\right\}^2}}{\omega k_{\min}\left(\alpha_f{}^2 \alpha_c (k_r + 1) - k_r\right)} \tag{8}$$

where k_{min} is defined as the required minimum ratio between V_{AC} and V_{OC}, reflecting the required AC voltage boost-up capability under all possible variations in α_v, α_r, α_f, and α_c.

3.1 System operating frequency variation

Depending on the design of primary power supplies, the operating frequency may drift which often causes significant power loss due to the mismatch in the resonant frequency between the primary and secondary sides. This is particularly a major concern in wireless power transfer systems using resonant variable frequency converters.

Figure 7 shows the effects of system operating frequency variation on AC voltage of the power pickup. It can be seen from the graph that the operating frequency is drifted with the variation so the tuned-point (T-P) is shifted accordingly. As for the magnitude of V_{AC}, it is also changed due to the tuning circuit requires different value of L_{S2} to achieve resonant condition and therefore resulted in various k_r. Note that there are two possible operating points for L_{S2} to compensate for the variations, and both of them are able to keep V_{AC} constant. However, depending on the design specifications, designer can choose to either work with the lower or higher inductance point.

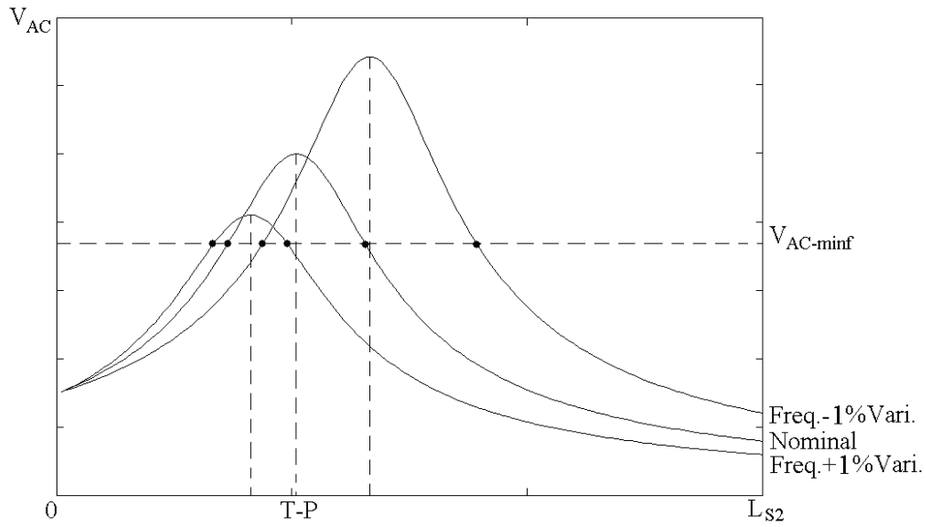

Fig. 7. The effect of system operating frequency variation on AC voltage of LCL power pickup.

3.2 Magnetic field coupling variation

The IPT system is normally involved in loosely coupled applications which allow free movements between the primary and secondary sides. In such applications, fluctuating open circuit voltage of the pickup coil is usually caused by coupling variations due to the free movements, and hence it needs to be compensated for keeping the output voltage constant.

Effect of the magnetic field coupling variation on AC voltage of the power pickup is shown in Fig. 8. It can be seen that the tuned-point and shape of the tuning circuit have both remained the same. Only the magnitude of open circuit voltage of the pickup coil has been changed and therefore resulted in different peak value of V_{AC}.

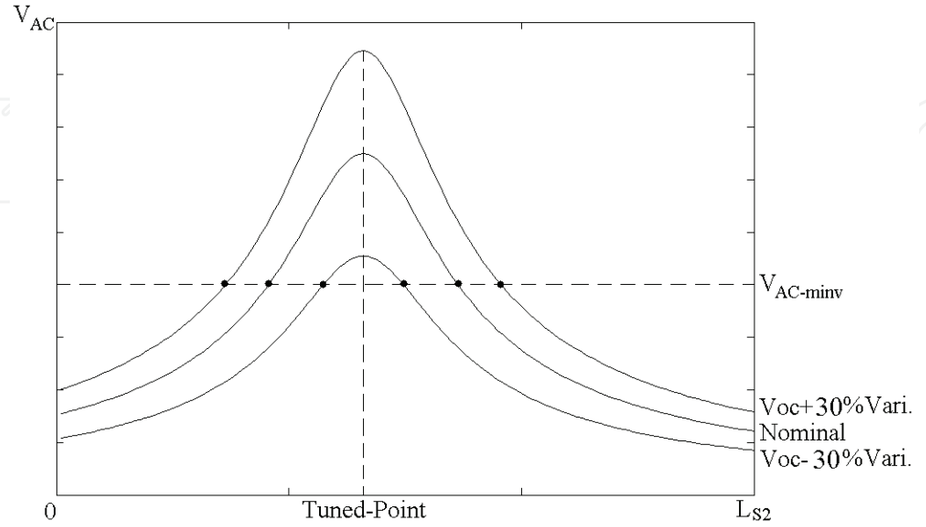

Fig. 8. The effect of magnetic coupling variation on AC voltage of LCL power pickup.

3.3 Load resistance variation

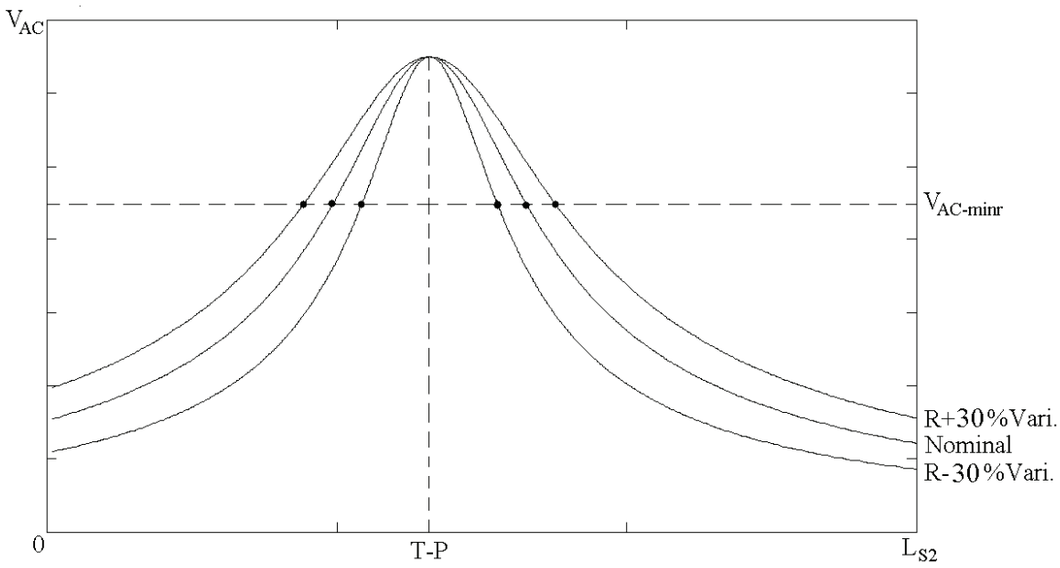

Fig. 9. The effect of load resistance variation on AC voltage of LCL power pickup.

Another variable whose effects need to be studied is the load resistance which varies as the loading condition changes. Fig. 9 shows the effect of load variation on V_{AC}. It can be seen from Fig. 9 that when the load increases, the sensitivity of V_{AC} with respect to L_{S2} decreases. On the contrary, when the load decreases, V_{AC} becomes very sensitive to the change of L_{S2}. These two results have indicated that when the power pickup is operating at extreme loading conditions, either L_{S2} will not be able to compensate for the variation, or the tuning circuit will be too sensitive with respect to L_{S2}.

3.4 Tuning capacitance variation

Unwanted variations of the tuning capacitor such as the variation caused by temperature change may result in undesired tuning condition change and affect the output voltage. This is particularly severe when the seondary system is working with high Q factor since the circuit becomes extremely sensitive to parameter variations.

Similar to the operating frequency variation, both the magnitude of peak V_{AC} and the T-P have been changed and shifted to different places after the variation as can be seen from Fig. 10. Note that as the tuning capacitance decreases/increases, the corresponding L_{S2} also needs to be increased/decreased to keep the circuit tuned, and this consequently causes the pickup to have different peak V_{AC} (or k_r).

3.5 Determination of range of the tuning inductance

In practical operations, the system operating frequency, magnetic coupling, and load resistance as well as other parameters may vary simultaneously. To design the variable capacitor and its controller properly, the worst-case maximum and minimum values of L_{S2} should be identified based on the integrated effect of concerned parameter variations to cover the full control range. Given the maximum allowed tolerance for each variation, the desired maximum and minimum inductance can be calculated by using (8), with the following conditions:

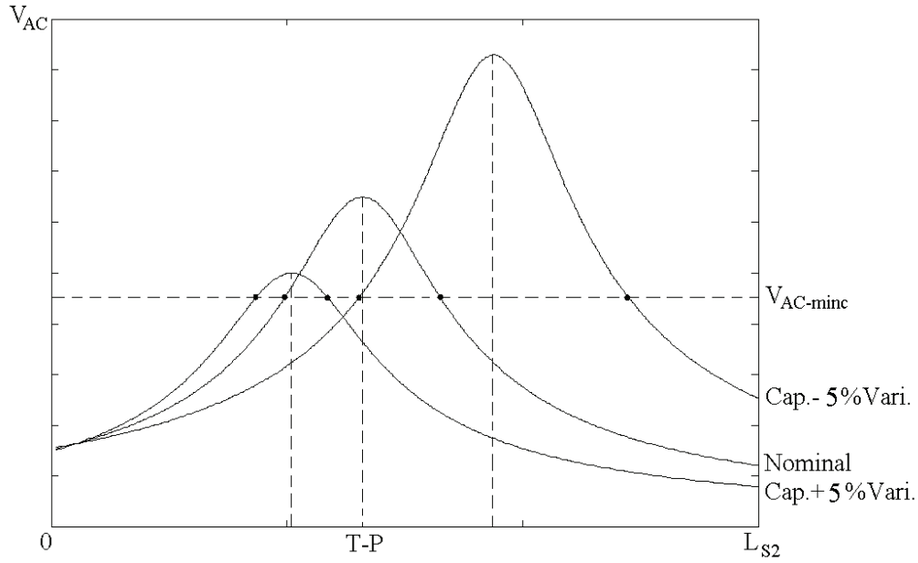

Fig. 10. The effect of tuning capacitor variation on ac voltage of power pick-up.

1. Maximum Inductance
   - Open circuit voltage, operating frequency, tuning capacitor, and load resistance are all at *Nominal value - maximum allowed tolerance*.
2. Minimum Inductance
   - Open circuit voltage, operating frequency, tuning capacitor, and load resistance are all at *Nominal value + maximum allowed tolerance*.

The method presented here can be extended to other possible parameter variations in the system for calculating the range of L_{S2} in worst-case scenario.

4. Design of Directional Tuning Control (DTC) algorithm

In both the shorting-control and dynamic tuning/detuning control method, traditional PI controller has been employed for their output voltage regulation and proven to be effective when the power pickup operates under single-side tuning condition. Nevertheless, it is practically difficult to maintain single-side operation, particularly for high Q systems. The system parameter variations may force the pickup to traverse from one operating region to the other region of the tuning curve and fail to control the output voltage. Directional Tuning Control (DTC) algorithm has been proposed to overcome the problems associated with full-range tuning of the power pickup. The fundamental concept of DTC is based on comparing the present value of control input with its immediate past value, and then use this result to determine the next control action. Instead of depending only on the output error detection as the traditional controllers do, the proposed controller generates the control signal based on the memory of previous control action following the procedure outlined in the flow chart of Fig. 11.

4.1 Standard procedure of DTC algorithm

The flow chart of DTC algorithm is shown in Fig. 11. Standard procedures of the DTC algorithm start with initializations. In this process, the controller initializes the settings

according to the user specifications, which include sampling time of the controller and initial state of each processing block. Since the algorithm is designed for controlling the power pick-up to focus on the steady state control, variation of the circuit time constant caused by other system parameter variations must be specified in the initial time delay of the program to avoid inaccurate sampling. After the initialisations, the output voltage at present-state V_{OUT}^{k} will be sampled, stored, and used to compare with a voltage reference V_{ref} and its previous stored value V_{OUT}^{k-1} for generating logic signals $S_1(k)$ and $S_2(k)$, respectively. These control signals are then collected by the next processing block to check with a predetermined truth table (Table 1) for determining the next-state control signal $S_4(k)$. Note that the memory block after the decision block stores the present control signal as $S_3(k)$, so it can later be used in the next execution for validity checking of the present control action.

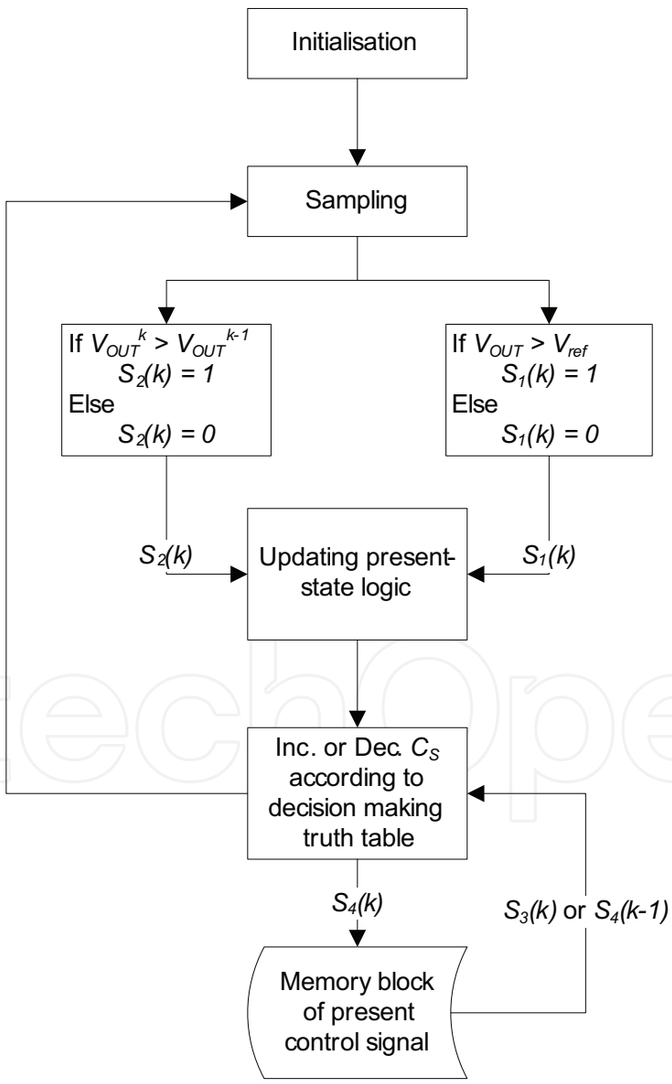

Fig. 11. Flow chart of the directional tuning control algorithm.

S_1	S_2	Previous –State (S_3)	Next-State (S_4)
0	0	0	1
0	0	1	0
0	1	0	0
0	1	1	1
1	0	0	0
1	0	1	1
1	1	0	1
1	1	1	0

Table 1. Truth table for L_{S2} increasing direction determination.

The simplified Boolean expression corresponding to Table I and the actual output signal of the controller can be expressed by:

$$S_4 = S_3(S_1 \oplus S_2) + \overline{S_3}(S_1 \equiv S_2) \tag{9}$$

$$U(k) = U(k-1) + (-1)^{S_4+1} \cdot \Delta h \tag{10}$$

where *U(k)* is the present-state control signal, *U(k-1)* is the previous-state control signal, and Δh is the step-size of the adjustment.

4.2 Fuzzy logic control for automatic selection of tuning step-size Δh

Despite the fact that the DTC algorithm can effectively control the output voltage of the pickup, the control quality is still restrained by the predefined tuning step-size. A larger step change in the inductance often causes chattering of the output voltage. Although the chattering effect can be reduced by using smaller step change in the inductance, it causes the overall response to be sluggish. To overcome the difficulties associated with the chattering problems and to make the overall response fast, a fuzzy logic controller is integrated with the classical DTC algorithm to further improve the performance of the controller (Hsu et al., 2008). The objective of the fuzzy logic controller is to dynamically determine the step change Δh of the tuning inductance in (10).

4.2.1 Fuzzification

Design of the fuzzy controller consists of fuzzification, formulation of control rule base, and defuzzification. In the process of fuzzification, operating region of the controller is designed to allow error and rate of error to lie inside a predetermined interval (-*L*, *L*). The inputs to the fuzzy PI controller are given as:

$$GE \cdot e(n) = GE \cdot [y_r(n) - y(n)] \tag{11}$$

$$GR \cdot r_1(n) = GR \cdot [e(n) - e(n-1)] \tag{12}$$

$$GR \cdot r_2(n) = GR \cdot [|e(n)| - |e(n-1)|] \tag{13}$$

where *y(n)* is the output voltage, $y_r(n)$is the reference signal, *e(n)* is the error signal, *GE* and *GR* are scaling factors for the error and the rate of error respectively. Since the rate of error is

calculated from values of output voltage at two consecutive sampling instances i.e. n and n-1, the rate of error *r(n)* has been further separated into two different variables $r_1(n)$ and $r_2(n)$, where $r_1(n)$ represents the rate of error when the output voltage at both these sampling instances i.e. y(n) and y(n-1) lie either above or below the reference value and $r_2(n)$ represents the rate of error when the output voltage at these two instances lie in different regions with respect to the reference value. The membership functions for error positive (e_p), error negative (e_n), rate positive (r_p), and rate negative (r_n) can be claculated from the following expressions:

$$\mu_{ep} = \frac{L + GE \cdot e(n)}{2L}, \quad \mu_{en} = \frac{L - GE \cdot e(n)}{2L} \tag{14}$$

$$\mu_{rp} = \frac{L + GR \cdot r(n)}{2L}, \quad \mu_{rn} = \frac{L - GR \cdot r(n)}{2L} \tag{15}$$

However, a simple fuzzy PI controller will fail to eliminate the chattering effect at the output voltage since the positive and negative errors calculated using (14) could be the same and cancel out with each other. Therefore a D controller is introduced here with a new set of inputs given by:

$$GD \cdot y_d(n) = GD \cdot \left| y_r(n) - y(n) \right| = GD \cdot \left| e(n) \right| \tag{16}$$

$$GM \cdot \Delta y(n) = GM \cdot \left| y(n) - y(n-1) \right| \tag{17}$$

where $y_d(n)$ is the absolute value of the error, $\Delta y(n)$ is the absolute value of the rate of output, *GD* and *GM* are scaling factors for the absolute error and the absolute rate of output respectively. The membership functions for absolute error large (y_{dl}), absolute error zero (y_{dz}), absolute rate of output large (Δy_l), and absolute rate of output zero (Δy_z) are given as:

$$\mu_{ydl} = \frac{GD \cdot y_d(n)}{L}, \quad \mu_{ydz} = 1 - \frac{GD \cdot y_d(n)}{L} \tag{18}$$

$$\mu_{\Delta yl} = \frac{GM \cdot \Delta y(n)}{L}, \quad \mu_{\Delta yz} = 1 - \frac{GM \cdot \Delta y(n)}{L} \tag{19}$$

4.2.2 Control rule base

The control rules for the normal tuning operation are as follows:

R_1: If *GE e(n)* is e_p and *GR r(n)* is r_{1p} Then $\Delta u_{PI}(n)$ is o_l.

R_2: If *GE e(n)* is e_p and *GR r(n)* is r_{1n} Then $\Delta u_{PI}(n)$ is o_z.

R_3: If *GE e(n)* is e_n and *GR r(n)* is r_{1p} Then $\Delta u_{PI}(n)$ is o_z.

R_4: If *GE e(n)* is e_n and *GR r(n)* is r_{1n} Then $\Delta u_{PI}(n)$ is o_l.

An extra set of four control rules for reducing the output chattering are:

R_5: If *GE e(n)* is e_p and *GR r(n)* is r_{2p} Then $\Delta u_{PI}(n)$ is o_l.

R_6: If *GE e(n)* is e_p and *GR r(n)* is r_{2n} Then $\Delta u_{PI}(n)$ is o_z.

R_7: If *GE e(n)* is e_n and *GR r(n)* is r_{2p} Then $\Delta u_{PI}(n)$ is o_l.

R_8: If *GE e(n)* is e_n and *GR r(n)* is r_{2n} Then $\Delta u_{PI}(n)$ is o_z.

The D controller considered here has only four control rules since it only takes the absolute value of the error and the rate of output as its inputs.

R_9: If *GD* $y_d(n)$ is y_{dl} and *GM* $\Delta y(n)$ is Δy_l Then $\Delta u_D(n)$ is o_z.

R_{10}: If *GD* $y_d(n)$ is y_{dl} and *GM* $\Delta y(n)$ is Δy_z Then $\Delta u_D(n)$ is o_z.

R_{11}: If *GD* $y_d(n)$ is y_{dz} and *GM* $\Delta y(n)$ is Δy_l Then $\Delta u_D(n)$ is o_l.

R_{12}: If *GD* $y_d(n)$ is y_{dz} and *GM* $\Delta y(n)$ is Δy_z Then $\Delta u_D(n)$ is o_l.

In the above rules, $\Delta u_{PI}(n)$ and $\Delta u_D(n)$ stands for crisp incremental output of the fuzzy PI controller and the fuzzy D controller respectively.

4.2.3 Defuzzificaction

Defuzzification of the output for fuzzy PI and fuzzy D controller is carried out by using center of gravity algorithm and are expressed as:

$$\Delta\mu_{1PI} = \frac{H \cdot S(\mu_{R_1R_4}) + 0 \cdot S(\mu_{R_2R_3})}{S(\mu_{R_1R_4}) + S(\mu_{R_2R_3})} \tag{20}$$

$$\Delta\mu_{2PI} = \frac{H \cdot S(\mu_{R_5R_7}) + 0 \cdot S(\mu_{R_6R_8})}{S(\mu_{R_5R_7}) + S(\mu_{R_6R_8})} \tag{21}$$

$$\Delta\mu_D = \frac{H \cdot S(\mu_{R_{11}R_{12}}) + 0 \cdot S(\mu_{R_9R_{10}})}{S(\mu_{R_{11}R_{12}}) + S(\mu_{R_9R_{10}})} \tag{22}$$

where the membership of output fuzzy sets for control rules R_1R_4, R_2R_3, R_5R_7, R_6R_8, R_9R_{10}, and $R_{11}R_{12}$ are obtained from Lukasewicz fuzzy logic, or, i.e. $\mu_{R_1R_4} = \min(\mu_{R_1} + \mu_{R_4}, 1)$. The function $S(\mu)$ is computed using Mamdani reference.

$$S(\mu) = \mu(2-\mu)H \tag{23}$$

The actual output of the controller which determines the tuning step-size for the variable capacitor is given by:

$$GU \cdot \Delta\mu = GU \cdot (\Delta\mu_{PI} - \Delta\mu_D) \tag{24}$$

where *GU* is a scaling factor for the crisp incremental output of the fuzzy PID controller.

5. Simulation results

To illustrate the effectiveness of the proposed fuzzy based DTC algorithm, a power pickup model has been created in MATLAB Simulink and PLECS.

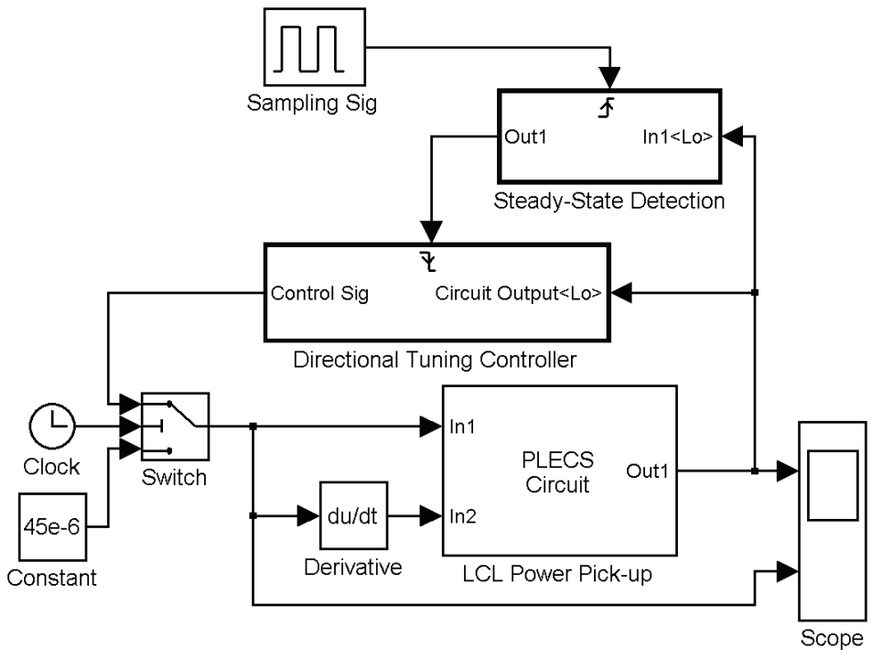

Fig. 12. Simulink model of LCL based power pickup with DTC.

The secondary power pickup model with DTC is shown in Fig. 12. Operating conditions of the power pickup can generally be categorized into four different cases such as: Under-Tuned with Low Start-up Voltage (UT-LSV), Under-Tuned with High Start-up Voltage (UT-HSV), Over-Tuned with Low Start-up Voltage (OT-LSV), and Over-Tuned with High Start-up Voltage (OT-HSV). However, their results are similar to each other during the control process and therefore only two of them are presented here.

The simulation result of V_{OUT}, and L_{S2}, are shown in Figure 13(a) and (b) respectively when the power pickup is operating under UT-LSV. The simulation was started from the circuit start-up with a predetermined delay of 0.05s (for separating the initialization and the actual control process, easing the observation) until it reaches the desired output voltage level (5V). As the error gets reduced, the step change in the tuning inductance also decreases to remove the output chattering effect.

Figure 14 shows the simulation results of the controlled power pickup operating under OT-HSV. As can be seen from the results, both UT-LSV and OT-HSV give similar outcome for providing a constant voltage at the output.

From the results of simulation studies of the controlled power pickup under different operating conditions, it was observed that the proposed controller is capable of controlling the output voltage to the desired value with a response time of 0.1~0.25s. However, the sampling frequency of the controller has to be selected carefully to achieve a more efficient output voltage regulation.

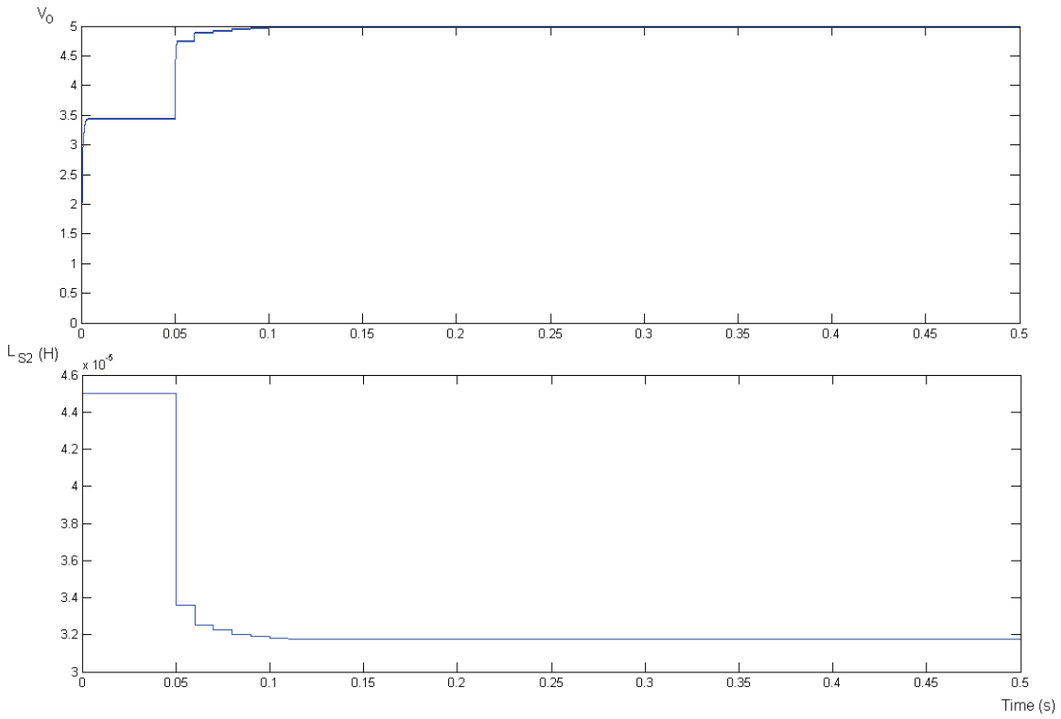

Fig. 13. Waveform of: a) output voltage of power pickup and b) tuning inductance, with Fuzzy based DTC algorithm controlled power pickup operating under UT-LSV.

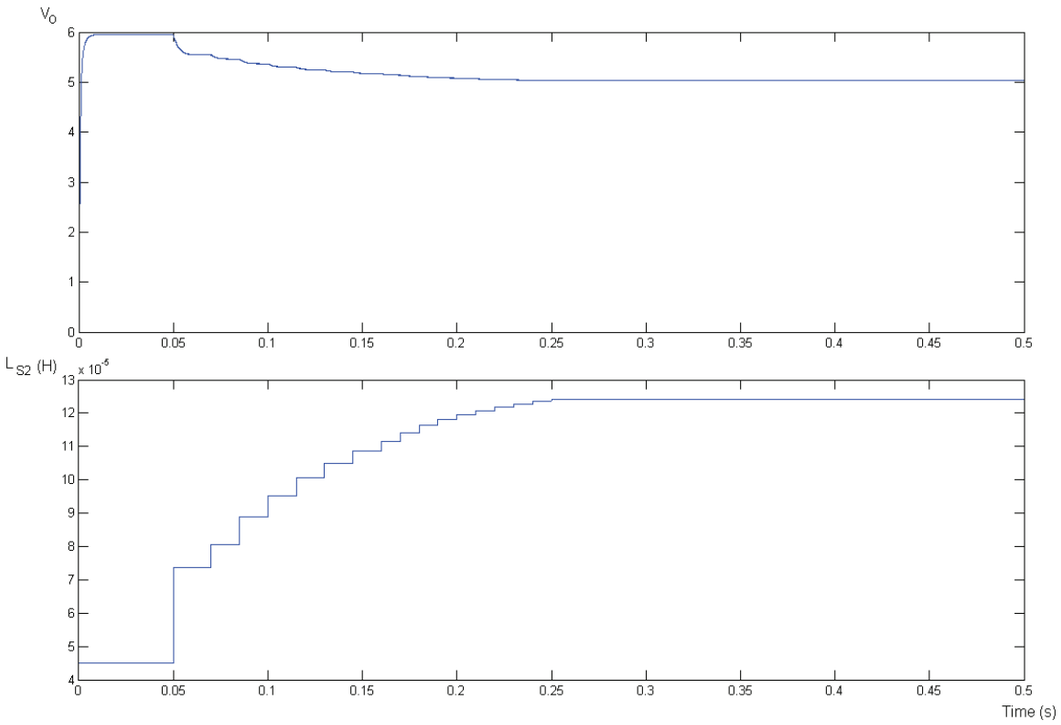

Fig. 14. Waveform of: a) output voltage of power pickup and b) tuning inductance, with Fuzzy based DTC algorithm controlled power pickup operating under OT-HSV.

6. Conclusions

A fuzzy based controller tuning step-size adjuster has been integrated with directional tuning controller to automatically determine the tuning step-size and to effectively regulate the output voltage of the power pickup for inductive power transfer system. The integrated controller has solved the directional tracking problem of the traditional PI dynamic tuning/detuning controller and hence achieved full-range power flow control of the secondary power pickup. The simulation performed by MATLAB Simulink and PLECS have demonstrated the effectiveness of the controller under different testing conditions and it has been shown that a desired constant output voltage can be maintained using the proposed controller without chattering effect. Within certain allowable tolerance of the pickup circuit parameters, the controller can automatically find the correct tuning directions. This helps to ease the circuit component selection in design and eliminates the tedious fine-tuning process in practical implementation.

7. Future research

As the fuzzy based directional tuning control algorithm is developed in discrete-time domain, sampling frequency becomes a very important factor which often affects the performance of the controller. Although the power pickup system will never go unstable since the output voltage is confined by the tuned-point, the true control result of each control action and the response time of the controller are still significantly affected by the sampling frequency. Two different aspects e.g. the magnitude of voltage variation after each control action and the time constant of the DC filter of the power pickup have been preliminarily investigated. However, a clear relationship between these two variables has not yet been found and therefore needs to be further explored.

8. References

T. Bieler, M. Perrottet, V. Nguyen, and Y. Perriard, "Contactless power and information transmission," *IEEE Transactions on Industry Applications*, vol. 26, no. 5, pp. 1266-1272, 2002.

J.T. Boys, G.A. Covic, and A.W. Green, "Stability and control of inductively coupled power transfer systems," *IEE Proceedings of Electric Power Applications*, vol. 147, no. 1, pp. 37-43, 2000.

Y.-H. Chao, J.-J. Shieh, C.-T. Pan, W.-C. Shen, and M.-P. Chen, "A primary-side control strategy for series-parallel loosely coupled inductive power transfer systems," in *ICIEA 2007 2nd IEEE Conference on Industrial Electronics and Applications*. May 23-25 2007.

G.A.J. Elliott, J.T. Boys, and A.W. Green. "Magnetically coupled systems for power transfer to electric vehicles," in *International Conference on Power Electronics and Drive Systems*, Feb 21-24 1995.

M.D. Feezor, F.Y. Sorrell, and P.R. Blankinship, "An interface system for autonomous undersea vehicles," *IEEE Journal of Oceanic Engineering*, vol. 26, no. 4, pp. 522-525, 2001.

J. Gao, "Inductive power transmission for untethered micro-robots," in *IECON 2005 32nd IEEE Annual Conference of Industrial Electronics Society*. Nov 6-10 2005.

R.R. Harrison, "Designing efficient inductive power links for implantable devices," in *ISCAS 2007 IEEE International Symposium on Circuits and Systems*. May 27-30 2007.

J.-U.W. Hsu, A.P. Hu, A. Swain, X. Dai, and Y. Sun, "A new contactless power pick-up with continuous variable inductor control using magnetic amplifier," in *PowerCon 2006 International Conference on Power System Technology*. Oct 2006.

J.-U.W. Hsu, A.P. Hu, and A. Swain, "Fuzzy based directional tuning controller for a wireless power pick-up," in *TENCON 2008 IEEE Region 10 Conference*, Nov 19-21 2008.

J.-U. Hsu, A.P. Hu, "Determining the variable inductance range for an LCL wireless power pick-up," in *EDSSC 2007 IEEE Conference on Electron Devices and Solid-State Circuits*, Dec 20-22 2007.

J.-U.W. Hsu, A.P. Hu, and A. Swain, "A wireless power pick-up based on directional tuning control of magnetic amplifier," in *IEEE Transactions on Industrial Electronics*, vol. 56, no. 7, pp. 2771-2781, 2009.

A.P. Hu, I.L.W. Kwan, C. Tan, and Y. Li, "A wireless battery-less computer mouse with super capacitor energy buffer," in *ICIEA 2007 2nd IEEE Conference on Industrial Electronics and Applications*. May 23-25 2007.

A.P. Hu and S. Hussmann, "Improved power flow control for contactless moving sensor applications," *IEEE Power Electronics Letters*, vol. 2, no. 4, pp. 135-138, 2004.

D.K. Jackson, S.B. Leeb, and S.R. Shaw, "Adaptive control of power electronic drives for servomechanical systems," *IEEE Transactions on Power Electronics*, vol. 15, no. 6, pp. 1045-1055, 2000.

C.-G. Kim, D.-H. Seo, J.-S. You, J.-H. Park, and B.H. Cho, "Design of a contactless battery charger for cellular phone," *IEEE Transactions on Industrial Electronics*, vol. 48, no. 6, pp. 1238-1247, 2001.

S. Raabe and G.A.J. Elliott, "A quadrature pickup for inductive power transfer systems," in *ICIEA 2007 2nd IEEE Conference on Industrial Electronics and Applications*. May 23-25 2007.

P. Si, A.P. Hu, S. Malpas, and D. Budgett, "Switching frequency analysis of dynamically detuned ICPT power pick-ups," in *PowerCon 2006 International Conference on Power System Technology*, Oct 2006.

C.-S. Wang, O.H. Stielau, and G.A. Covic, "Load models and their application in the design of loosely coupled inductive power transfer systems," in *PowerCon 2000 International Conference on Power System Technology*. Dec 4-7 2000.

C.-S. Wang, O.H. Stielau, and G.A. Covic, "Design considerations for a contactless electric vehicle battery charger," *IEEE Transactions on Industrial Electronics*, vol. 52, no. 5, pp. 1308-1314, 2005.

L. Wang, M. Chen, and D. Xu, "Increasing inductive power transferring efficiency for maglev emergency power supply," in *PESC 2006 37th IEEE Power Electronics Specialists Conference*. Jun 18-22 2006.

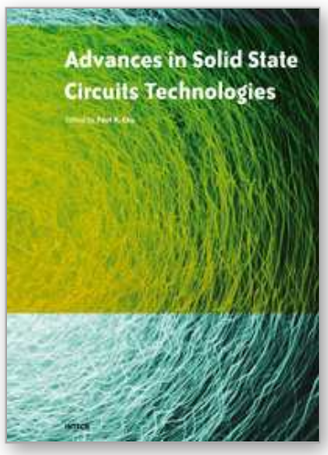

Advances in Solid State Circuit Technologies

Edited by Paul K Chu

ISBN 978-953-307-086-5
Hard cover, 446 pages
Publisher InTech
Published online 01, April, 2010
Published in print edition April, 2010

This book brings together contributions from experts in the fields to describe the current status of important topics in solid-state circuit technologies. It consists of 20 chapters which are grouped under the following categories: general information, circuits and devices, materials, and characterization techniques. These chapters have been written by renowned experts in the respective fields making this book valuable to the integrated circuits and materials science communities. It is intended for a diverse readership including electrical engineers and material scientists in the industry and academic institutions. Readers will be able to familiarize themselves with the latest technologies in the various fields.

How to reference

In order to correctly reference this scholarly work, feel free to copy and paste the following:

Jr-Uei William Hsu, Aiguo Patrick Hu and Akshya Swain (2010). Directional Tuning Control of Wireless/Contactless Power Pickup for Inductive Power Transfer (IPT) System, Advances in Solid State Circuit Technologies, Paul K Chu (Ed.), ISBN: 978-953-307-086-5, InTech, Available from: http://www.intechopen.com/books/advances-in-solid-state-circuit-technologies/directional-tuning-control-of-wireless-contactless-power-pickup-for-inductive-power-transfer-ipt-sys

INTECH
open science | open minds

InTech Europe
University Campus STeP Ri
Slavka Krautzeka 83/A
51000 Rijeka, Croatia
Phone: +385 (51) 770 447
Fax: +385 (51) 686 166
www.intechopen.com

InTech China
Unit 405, Office Block, Hotel Equatorial Shanghai
No.65, Yan An Road (West), Shanghai, 200040, China
中国上海市延安西路65号上海国际贵都大饭店办公楼405单元
Phone: +86-21-62489820
Fax: +86-21-62489821

IntechOpen